Postbuckling of Long Orthotropic Plates in Combined Shear and Compression

Manuel Stein*
NASA Langley Research Center, Hampton, Virginia

Von Kármán's nonlinear, large-deflection partial differential equations for orthotropic plates loaded in combined shear and compression are converted into a set of first-order nonlinear, ordinary differential equations by assuming trigonometric functions in one direction. These equations are solved numerically using a two-point boundary problem solver that makes use of Newton's method. Results are obtained that determine the postbuckling behavior of rectangular plates with loadings up to about three times the buckling load. Both isotropic and orthotropic composite plates are considered. The results show that orthotropic plates may behave quite differently than isotropic plates and that in-plane boundary conditions are important for plates loaded in shear.

Introduction

To take advantage of orthotropic plates having various extensional and bending properties, design methods need to be established for a variety of structural configurations and loadings. One of the basic elements in a structure is the rectangular flat plate supported at its edges. Because the structure is often subjected to combinations of loads, attention has been given to the problem of the plates buckling under more than one type of loading. Nondimensional parameters have been found (e.g., see Ref. 1) that allow buckling results to be presented as a series of curves on one plot covering the complete range of dimensions and material properties.

Although the level of loading that causes buckling is important, supported plates may carry a considerable load beyond buckling. Of interest is the response of a buckled plate to various kinds of additional loads, including those not previously applied. Postbuckling behavior can be obtained for many plate configurations using a general-purpose computer program such as that described in Ref. 2. Having nondimensional parameters is desirable, such that each of the loads and deformations of interest are calculated for a wide range of dimensions and material properties. The results are then presented in a set of curves. The designer could then determine the postbuckling behavior of any given panel by interpolation and simple calculations and thus determine the optimum panel that satisfies his needs. To make it economically feasible to calculate the values to present in this set of curves, a special-purpose program may be needed rather than a general-purpose one.

In Ref. 3, the large-deflection equations of von Kármán were written for specially orthotropic plates. Upon manipulation of the equations, it was found that only two new parameters beyond those required for buckling were needed to establish postbuckling behavior. Results for orthotropic plates loaded in compression are presented in Ref. 3, which shows that only one new parameter is needed for the postbuckling of long plates in compression. The other parameter is associated with shear stresses; so, the other parameter will be needed with any loading that involves shearing.

The purpose of this paper is to present the method of analysis and postbuckling results for long plates in combined compression and shear. Results are also presented for long plates loaded in shear alone and in compression alone, as well as for the shear stiffness of a plate buckled in compression alone and the compressive stiffness of a plate buckled in shear alone.

An extension of the method of Ref. 3 is used to obtain the results in this paper. In this method, the von Kármán nonlinear partial differential equations are converted into nonlinear ordinary differential equations by assuming trigonometric functions in one direction. These equations are then solved numerically using the method of Ref. 4 in a special-purpose computer program that is much more efficient than the available general-purpose computer programs for similar calculations. The effects of change in the buckle pattern are included in the calculations.

Analysis

Buckling of rectangular plates loaded in shear and compression is permitted before the ultimate load is reached in many structures, because the buckled plate retains much of the stiffness that it had before buckling. Postbuckling plate theory must be used to investigate the structural behavior between buckling and ultimate load. Of course, buckling results must be known before the postbuckling behavior can be found. Some recent buckling results for composite plates are presented in Refs. 1, 5, and 6. The present analysis uses a method of analysis for postbuckling problems different from that used previously (e.g., see Refs. 7-13).

Choice of Series for Displacements

Nonlinear ordinary differential equations are derived based on trigonometric series approximation for the displacements. The most important terms in the trigonometric series for postbuckling in compression were indicated by the perturbation method of Ref. 10.

The choice of the trigonometric term used for the analysis of long plates loaded in combined longitudinal compression and in-plane shear will now be discussed.

A sketch of the buckled plate under combined shear and compression is shown in Fig. 1. The plate has a width b and a half-wavelength λ in the y and x directions, respectively. At the ends, compressive displacements $\bar{u}_{cn}/2$ are applied and, at the long edges, $y=0$, b shearing displacements $\bar{u}_{sh}/2$ are applied. The out-of-plane deflection w is zero at the nodes of the

Presented as Paper 83-0876 at the AIAA/ASME/ASCE/AHS 24th Structures, Structural Dynamics and Materials Conference, Lake Tahoe, Nev., May 2-4, 1983; received June 20, 1983; revision received Jan. 16, 1984. This paper is declared a work of the U.S. Government and therefore is in the public domain.

*Senior Aerospace Engineer, Structural Mechanics Branch, Structures and Dynamics Division. Associate Fellow AIAA.

buckle pattern (every half-wavelength) and is zero at the edges $y=0, b$.

At buckling the equation for w for compression alone is satisfied by

$$w_s(y)\sin(\pi x/\lambda)$$

and the equations for u and v for compression alone are satisfied by

$$-\bar{u}_{cn}\left(\frac{x}{a}-\frac{1}{2}\right) \qquad \bar{v}_0\left(\frac{y}{b}-\frac{1}{2}\right)$$

where a is the plate length.

At buckling, the deflection pattern for shear alone is skewed with a half-wavelength λ in the longitudinal (x) direction and the equations for w are satisfied by[14]

$$w_s(y)\sin(\pi x/\lambda)+w_c(y)\cos(\pi x/\lambda)$$

where subscripts s and c refer to sine and cosine, respectively. This expression is general enough to include the compression buckling mode as a special case and is, therefore, applicable to buckling under combined shear and compression. The equations for u and v for shear alone are satisfied by

$$\bar{u}_{sh}\,[\,(y/b)-\tfrac{1}{2}\,]$$

$$0$$

The postbuckling study of Ref. 10, which solves for the unknowns in order of their importance (the perturbation method) for compression alone, indicates that the next group of terms to be considered are

$$u_s(y)\sin(2\pi x/\lambda) \qquad v_c(y)\cos(2\pi x/\lambda)$$

and then,

$$w_{3s}(y)\sin(3\pi x/\lambda)$$

However, the coefficient w_{3s} was found to be small compared to w_s for a long plate.

The choice of the next group of trigonometric terms to use for the problem of shear alone or of combined shear and compression is not as straightforward as for that of compression alone. Guided by the experimental and theoretical results for shear, which indicate that the buckle mode does not change much in the initial postbuckling range, the postbuckling response in combined shear and compression may be given by the combined shear and compression buckling mode and a few elementary terms beyond. Accordingly, the displacements for this problem are taken to be

$$u=-\bar{u}_{cn}\left(\frac{x}{a}-\frac{1}{2}\right)+u_0(y)+u_s(y)\sin\frac{2\pi x}{\lambda}+u_c(y)\cos\frac{2\pi x}{\lambda}$$

$$v=v_0(y)+v_s(y)\sin\frac{2\pi x}{\lambda}+v_c(y)\cos\frac{2\pi x}{\lambda}$$

$$w=w_s(y)\sin\frac{\pi x}{\lambda}+w_c(y)\cos\frac{\pi x}{\lambda} \tag{1}$$

The deflection w, which is exact at buckling, is sinusoidally periodic with half-wavelength λ. The displacements u and v are sinusoidally periodic with half-wavelength $\lambda/2$ and u has an extra, linear-in-x term associated with the constant $\bar{u}_{cn}$, which is specified. Specifying $\bar{u}_{cn}$ identifies the applied longitudinal compressive displacement. The applied shearing displacement $\bar{u}_{sh}$ is specified through the boundary conditions on $u_0(y)$.

Derivation of Differential Equations

The neutral surface strains and curvatures as given by von Kármán are

$$\epsilon_x=u_{,x}+\tfrac{1}{2}w_{,x}^2 \qquad K_x=-w_{,xx}$$

$$\epsilon_y=v_{,y}+\tfrac{1}{2}w_{,y}^2 \qquad K_y=-w_{,yy}$$

$$\gamma_{xy}=u_{,y}+v_{,x}+w_{,x}w_{,y} \qquad K_{xy}=-2w_{,xy}$$

By substitution from Eq. (1), the strains and curvatures are of the form

$$\epsilon_x=\epsilon_{x0}(y)+\epsilon_{xs}(y)\sin\frac{2\pi x}{\lambda}+\epsilon_{xc}(y)\cos\frac{2\pi x}{\lambda}$$

$$\epsilon_y=\epsilon_{y0}(y)+\epsilon_{ys}(y)\sin\frac{2\pi x}{\lambda}+\epsilon_{yc}(y)\cos\frac{2\pi x}{\lambda}$$

$$\gamma_{xy}=\gamma_{xy0}(y)+\gamma_{xys}(y)\sin\frac{2\pi x}{\lambda}+\gamma_{xyc}(y)\cos\frac{2\pi x}{\lambda}$$

$$K_x=K_{xs}(y)\sin\frac{\pi x}{\lambda}+K_{xc}(y)\cos\frac{\pi x}{\lambda}$$

$$K_y=K_{ys}(y)\sin\frac{\pi x}{\lambda}+K_{yc}(y)\cos\frac{\pi x}{\lambda}$$

$$K_{xy}=K_{xys}(y)\sin\frac{\pi x}{\lambda}+K_{xyc}(y)\cos\frac{\pi x}{\lambda} \tag{2}$$

where

$$\epsilon_{x0}=-\frac{\bar{u}_{cn}}{a}+\frac{1}{4}\left(\frac{\pi}{\lambda}\right)^2(w_s^2+w_c^2)$$

$$\epsilon_{xs}=-\frac{2\pi}{\lambda}u_c-\frac{1}{2}\left(\frac{\pi}{\lambda}\right)^2 w_s w_c$$

$$\epsilon_{xc}=\frac{2\pi}{\lambda}u_s+\frac{1}{4}\left(\frac{\pi}{\lambda}\right)^2(w_s^2-w_c^2)$$

$$\epsilon_{y0}=v_0'+\tfrac{1}{4}(w_s'^2+w_c'^2)$$

$$\epsilon_{ys}=v_s'+\tfrac{1}{2}w_s'w_c'$$

$$\epsilon_{yc}=v_c'+\tfrac{1}{4}(-w_s'^2+w_c'^2)$$

$$\gamma_{xy0}=u_0'+\frac{1}{2}\frac{\pi}{\lambda}(w_s w_c'-w_c w_s')$$

$$\gamma_{xys}=u_s'-\frac{2\pi}{\lambda}v_c+\frac{1}{2}\frac{\pi}{\lambda}(w_s w_s'-w_c w_c')$$

$$\gamma_{xyc}=u_c'+\frac{2\pi}{\lambda}v_s+\frac{1}{2}\frac{\pi}{\lambda}(w_s w_c'+w_c w_s') \tag{3}$$

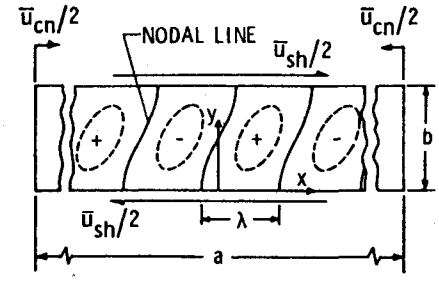

Fig. 1 Buckled plate under combined shear and compression.

$$K_{xs}=(\pi/\lambda)^2 w_s,\quad K_{xc}=(\pi/\lambda)^2 w_c,\quad K_{ys}=-w_s''$$

$$K_{yc}=-w_c'',\quad K_{xys}=2(\pi/\lambda)w_c',\quad K_{xyc}=-2(\pi/\lambda)w_s'$$

The prime ($'$) indicates a derivative with respect to y. From the stress-strain relations for an orthotropic plate, the stress and moment resultants are

$$N_x=A_{11}\epsilon_x+A_{12}\epsilon_y \qquad M_x=D_{11}K_x+D_{12}K_y$$

$$N_y=A_{22}\epsilon_y+A_{12}\epsilon_x \qquad M_y=D_{22}K_y+D_{12}K_x$$

$$N_{xy}=A_{66}\gamma_{xy} \qquad M_{xy}=D_{66}K_{xy} \tag{4}$$

The form of the stress and moment resultants in terms of the trigonometric terms in the x direction with coefficients functions of y is similar to the form of the strains.

The virtual work of the system is

$$\delta\Pi=\int_0^b\int_0^\lambda (N_x\delta\epsilon_x+N_y\delta\epsilon_y+N_{xy}\delta\gamma_{xy}+M_x\delta K_x+M_y\delta K_y+M_{xy}\delta K_{xy})\,dx\,dy \tag{5}$$

Substituting Eq. (2) into Eq. (5) and integrating over x results in

$$\delta\Pi=\frac{\lambda}{2}\int_0^b (2N_{x0}\delta\epsilon_{x0}+N_{xs}\delta\epsilon_{xs}+N_{xc}\delta\epsilon_{xc}+2N_{y0}\delta\epsilon_{y0}+N_{ys}\delta\epsilon_{ys}+N_{yc}\delta\epsilon_{yc}+2N_{xy0}\delta\gamma_{xy0}+N_{xys}\delta\gamma_{xys}+N_{xyc}\delta\gamma_{xyc}+M_{xs}\delta K_{xs}+M_{xc}\delta K_{xc}+M_{ys}\delta K_{ys}+M_{yc}\delta K_{yc}+M_{xys}\delta K_{xys}+M_{xyc}\delta K_{xyc})\,dy \tag{6}$$

Substituting Eq. (2) into Eq. (6) and integrating by parts leads to

$$\begin{aligned}\delta\Pi=\frac{\lambda}{2}\int_0^b \Big\{&-2N'_{xy0}\delta u_0+\left(-N'_{xys}+\frac{2\pi}{\lambda}N_{xc}\right)\delta u_s\\&+\left(-N'_{xyc}-\frac{2\pi}{\lambda}N_{xs}\right)\delta u_c-2N'_{y0}\delta v_0\\&+\left(-N'_{ys}+\frac{2\pi}{\lambda}N_{xyc}\right)\delta v_s+\left(-N'_{yc}-\frac{2\pi}{\lambda}N_{xys}\right)\delta v_c\\&+\left[-Q'_s+(2N_{x0}w_s-N_{xs}w_c+N_{xc}w'_s)\frac{1}{2}\left(\frac{\pi}{\lambda}\right)^2\right.\\&\left.+(2N_{xy0}\beta_c+N_{xys}\beta_s+N_{xyc}\beta_c)\frac{1}{2}\frac{\pi}{\lambda}+M_{xs}\left(\frac{\pi}{\lambda}\right)^2\right]\delta w_s\\&+\left[-Q'_c+(2N_{x0}w_c-N_{xs}w_s-N_{xc}w_c)\frac{1}{2}\left(\frac{\pi}{\lambda}\right)^2\right.\\&+(-2N_{xy0}\beta_s-N_{xys}\beta_c+N_{xyc}\beta_s)\frac{1}{2}\frac{\pi}{\lambda}\\&\left.+M_{xc}\left(\frac{\pi}{\lambda}\right)^2\right]\delta w_c\Big\}dy+\frac{\lambda}{2}(2N_{xy0}\delta u_0+N_{xys}\delta u_s\\&+N_{xyc}\delta u_c+2N_{y0}\delta v_0+N_{ys}\delta v_s+N_{yc}\delta v_c+Q_s\delta w_s\\&+Q_c\delta w_c-M_{ys}\delta\beta_s-M_{yc}\delta\beta_c)_0^b\end{aligned} \tag{7}$$

where, by definition,

$$\begin{aligned}Q_s=&(2N_{y0}\beta_s+N_{ys}\beta_c-N_{yc}\beta_s)\tfrac{1}{2}+(-2N_{xy0}w_c\\&+N_{xys}w_s+N_{xyc}w_c)\frac{1}{2}\frac{\pi}{\lambda}+M'_{ys}-2M_{xyc}\frac{\pi}{\lambda}\end{aligned}$$

$$\begin{aligned}Q_c=&(2N_{yo}\beta_c+N_{ys}\beta_s+N_{yc}\beta_c)\tfrac{1}{2}+(2N_{xy0}w_s-N_{xys}w_c\\&+N_{xyc}w_s)\frac{1}{2}\frac{\pi}{\lambda}+M'_{yc}+2M_{xys}\frac{\pi}{\lambda}\end{aligned}$$

$$\beta_s=w'_s,\quad \beta_c=w'_c \tag{8}$$

Thus, the principle of virtual work requires satisfaction of the following differential equations and choice of boundary conditions:

$$N'_{xy0}=0 \qquad N'_{xys}=\frac{2\pi}{\lambda}N_{xc} \qquad N'_{xyc}=-\frac{2\pi}{\lambda}N_{xs}$$

$$N'_{y0}=0 \qquad N'_{ys}=\frac{2\pi}{\lambda}N_{xyc} \qquad N'_{yc}=-\frac{2\pi}{\lambda}N_{xys}$$

$$\begin{aligned}Q'_s=&(2N_{x0}w_s-N_{xs}w_c+N_{xc}w_s)\frac{1}{2}\left(\frac{\pi}{\lambda}\right)^2\\&+(2N_{xy0}\beta_c+N_{xys}\beta_s+N_{xyc}\beta_c)\frac{1}{2}\frac{\pi}{\lambda}+M_{xs}\left(\frac{\pi}{\lambda}\right)^2\end{aligned}$$

$$\begin{aligned}Q'_c=&(2N_{x0}w_c-N_{xs}w_s-N_{xc}w_c)\frac{1}{2}\left(\frac{\pi}{\lambda}\right)^2\\&+(-2N_{xy0}\beta_s-N_{xys}\beta_c+N_{xyc}\beta_s)\frac{1}{2}\frac{\pi}{\lambda}+M_{xc}\left(\frac{\pi}{\lambda}\right)^2\end{aligned}$$

$$(N_{xy0}\delta u_0)_0^b=0 \qquad (N_{xys}\delta u_s)_0^b=0 \qquad (N_{xyc}\delta u_c)_0^b=0$$

$$(N_{y0}\delta v_0)_0^b=0 \qquad (N_{ys}\delta v_s)_0^b=0 \qquad (N_{yc}\delta v_c)_0^b=0$$

$$(Q_s\delta w_s)_0^b=0 \qquad (Q_c\delta w_c)_0^b=0$$

$$(M_{ys}\delta\beta_s)_0^b=0 \qquad (M_{yc}\delta\beta_c)_0^b=0 \tag{9}$$

The boundary conditions assumed for the results presented in this paper are that the edges are simply supported and held straight. The edge at $y=0$ is displaced relative to the edge at $y=b$ to give a specified (applied) shearing displacement; also, v_0 must be set equal to zero at some value of y to prevent translation in the y direction. These boundary conditions are expressed as

1) Simply supported at $y=0$, b:

$$w_s=w_c=M_{xs}=M_{xc}=0$$

2) Straight edges at $y=0$, b:

$$u_s=u_c=v_s=v_c=0$$

3) Applied shearing displacement at

$$y=0: \qquad u_0=-\bar{u}_{sh}/2$$

$$y=b: \qquad u_0=\bar{u}_{sh}/2$$

$$y=b/2: \qquad v_0=0$$

In addition, the average direct force across the width is zero,

$$\frac{1}{2\lambda b}\int_0^b\int_0^{2\lambda} N_y\,dx\,dy = 0$$

The unkown N_{y0} is solved directly. From Eqs. (9), N_{y0} is constant and, from the above condition, $N_{y0}=0$ everywhere.

The system of first-order ordinary differential equations to be solved for this problem are presented in terms of the 18 unknowns

$$u_0,\ u_s,\ u_c,\ v_s,\ v_c,\ w_s,\ w_c,\ \beta_s,\ \beta_c$$

$$N_{xy0},\ N_{xys},\ N_{xyc},\ N_{ys},\ N_{yc},\ Q_s,\ Q_c,\ M_{ys},\ M_{yc}$$

Equations (9), which were obtained from the virtual work, present seven of the equations in the differential system used (excluding the N_{y0} equation). Equations (10) were obtained from the stress-strain relations [Eqs. (4)] using Eqs. (2), (3), and (8); they present seven more differential equations,

$$u_0' = -\frac{1}{2}\frac{\pi}{\lambda}(w_s\beta_c - w_c\beta_s) + \frac{N_{xy0}}{A_{66}}$$

$$u_s' = \frac{2\pi}{\lambda}v_c - \frac{1}{2}\frac{\pi}{\lambda}(w_s\beta_s - w_c\beta_c) + \frac{N_{xys}}{A_{66}}$$

$$u_c' = -\frac{2\pi}{\lambda}v_s - \frac{1}{2}\frac{\pi}{\lambda}(w_s\beta_c + w_c\beta_s) + \frac{N_{xyc}}{A_{66}}$$

$$v_s' = -\frac{1}{2}\beta_s\beta_c + \frac{A_{12}}{A_{22}}\left[\frac{2\pi}{\lambda}u_c + \frac{1}{2}\left(\frac{\pi}{\lambda}\right)^2 w_s w_c\right] + \frac{N_{ys}}{A_{22}}$$

$$v_c' = \frac{1}{4}(\beta_s^2-\beta_c^2) - \frac{A_{12}}{A_{22}}\left[\frac{2\pi}{\lambda}u_s + \frac{1}{4}\left(\frac{\pi}{\lambda}\right)^2(w_s^2-w_c^2)\right] + \frac{N_{yc}}{A_{22}}$$

$$\beta_s' = (D_{12}/D_{22})(\pi/\lambda)^2 w_s - M_{ys}/D_{22}$$

$$\beta_c' = (D_{12}/D_{22})(\pi/\lambda)^2 w_c - M_{yc}/D_{22} \qquad (10)$$

Four differential equations result from Eqs. (8)

$$w_s' = \beta_s \qquad w_c' = \beta_c$$

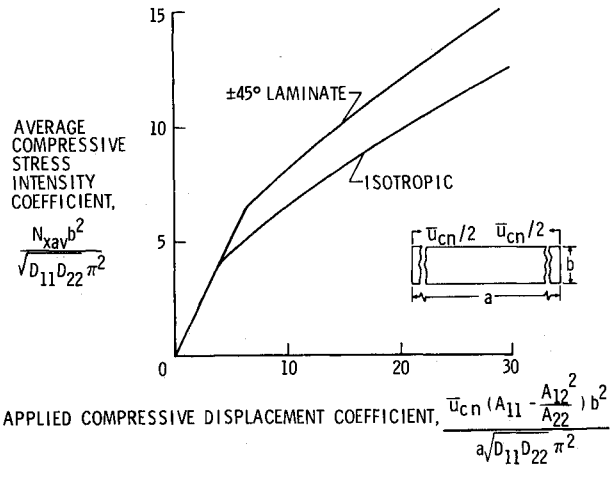

Fig. 2 Characteristic curves for long plates with simply supported straight edges and loaded in longitudinal compression.

$$M_{ys}' = Q_s - (2N_{y0}\beta_s + N_{ys}\beta_c - N_{yc}\beta_s)\tfrac{1}{2} - (-2N_{xy0}w_c + N_{xys}w_s + N_{xyc}w_c)\frac{1}{2}\frac{\pi}{\lambda} + M_{xyc}\frac{2\pi}{\lambda}$$

$$M_{yc}' = Q_c - (2N_{y0}\beta_c + N_{ys}\beta_s + N_{yc}\beta_c)\tfrac{1}{2} - (2N_{xy0}w_s - N_{xys}w_c + N_{xyc}w_s)\frac{1}{2}\frac{\pi}{\lambda} - M_{xys}\frac{2\pi}{\lambda} \qquad (11)$$

The following additional relations are needed; they were also obtained from the stress-strain relations [Eqs. (4)] using Eqs. (2), (3), and (8):

$$N_{x0} = \left(A_{11} - \frac{A_{12}^2}{A_{22}}\right)\left[-\frac{\bar{u}_{cn}}{a} + \frac{1}{4}\left(\frac{\pi}{\lambda}\right)^2(w_s^2+w_c^2)\right] + \left(\frac{A_{12}}{A_{22}}\right)N_{y0}$$

$$N_{xs} = -\left(A_{11} - \frac{A_{12}^2}{A_{22}}\right)\left[u_c\frac{2\pi}{\lambda} + \frac{1}{2}\left(\frac{\pi}{\lambda}\right)^2 w_s w_c\right] + \left(\frac{A_{12}}{A_{22}}\right)N_{ys}$$

$$N_{xc} = \left(A_{11} - \frac{A_{12}^2}{A_{22}}\right)\left[u_s\frac{2\pi}{\lambda} + \frac{1}{4}\left(\frac{\pi}{\lambda}\right)^2(w_s^2-w_c^2)\right] + \left(\frac{A_{12}}{A_{22}}\right)N_{yc}$$

$$M_{xs} = \left(D_{11} - \frac{D_{12}^2}{D_{22}}\right)\left(\frac{\pi}{\lambda}\right)^2 w_s + \left(\frac{D_{12}}{D_{22}}\right)M_{ys}$$

$$M_{xc} = \left(D_{11} - \frac{D_{12}^2}{D_{22}}\right)\left(\frac{\pi}{\lambda}\right)^2 w_c + \left(\frac{D_{12}}{D_{22}}\right)M_{yc}$$

$$M_{xys} = (2\pi/\lambda)D_{66}\beta_c$$

$$M_{xyc} = -(2\pi/\lambda)D_{66}\beta_s \qquad (12)$$

One equation from the stress-strain relations has not been used yet. It is a first-order differential equation for v_0,

$$v_0' = -\frac{1}{4}(\beta_s^2+\beta_c^2) - \frac{A_{12}}{A_{22}}\left[-\frac{\bar{u}_{cn}}{a} + \frac{1}{4}\left(\frac{\pi}{\lambda}\right)^2(w_s^2+w_c^2)\right] + \frac{N_{y0}}{A_{22}}$$

This equation permits a solution for v_0 after the rest of the equations have been solved.

In summary, by using simplifying assumptions, nonlinear ordinary differential equations have been derived from basic relations to replace the nonlinear partial differential equations of plate theory. The derivation employed the principle of virtual work in conjunction with the assumption that the displacements are represented by the first few terms of a Fourier series. Solution of the ordinary differential equations, subject to the boundary conditions that arise naturally in the derivation, is obtained using the algorithm described in the next subsection.

Solution Technique

An algorithm based on Newton's method has been developed by Lentini and Pereyra[4] to solve a system of simultaneous first-order nonlinear ordinary differential equations subject to two-point conditions. The system of equations

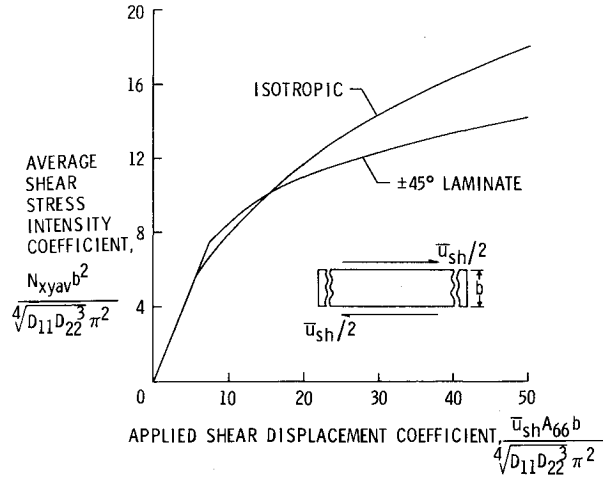

Fig. 3 Characteristic curves for long plates with simply supported straight edges and loaded in shear.

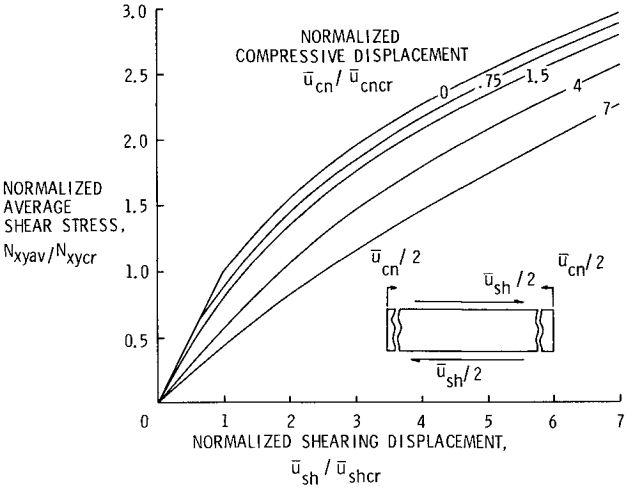

Fig. 4 Average shear stress for an isotropic simply supported plate with edges straight subject to shearing and longitudinal compressive displacements.

is of the form

$$\bar{y}' = \bar{F}(x,\bar{y})$$

where $\bar{y}$ is the vector of dependent variables and x is the independent variable defined in the interval (a,b). The boundary conditions of the problem are specified by

$$\bar{g}[\bar{y}(a),\ \bar{y}(b)] = 0$$

This algorithm uses finite differences with deferred corrections, and adaptive mesh spacings are automatically produced so that mild boundary layers are detected and resolved.

Applications

This paper presents results for a long, simply supported plate with straight edges loaded in combined in-plane shear and longitudinal compression beyond its buckling load. For given values of the applied displacements $\bar{u}_{cn}$ and $\bar{u}_{sh}$ and for prescribed values of the dimensions, material properties, and half-wavelength λ, the system of equations may be solved and the average compressive stress intensity and shear stress intensity may be determined, where the average stress intensities are

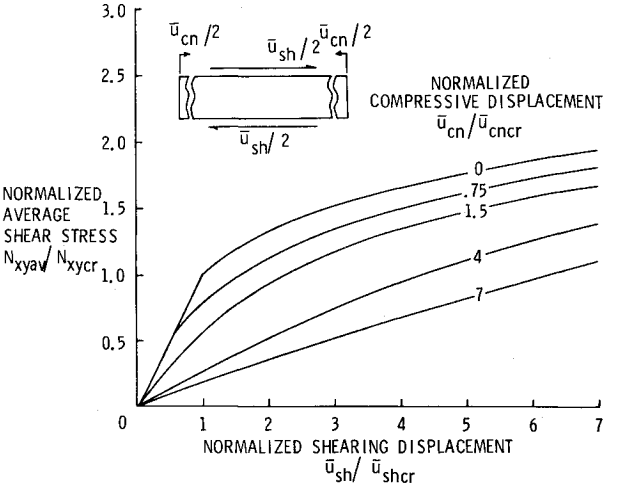

Fig. 5 Average shear stress for ±45 deg laminated composite simply supported plate with edges straight subject to shearing and longitudinal compressive displacements.

$$N_{xav} = -\frac{1}{2\lambda b}\int_0^b\int_0^{2\lambda} N_x\,dx\,dy = -\frac{1}{b}\int_0^b N_{x0}\,dy$$

$$N_{xyav} = \frac{1}{2\lambda b}\int_0^b\int_0^{2\lambda} N_{xy}\,dx\,dy = N_{xy0}$$

The wavelength of interest is the one that corresponds to minimum energy and the solution of interest is on the equilibrium path that gives nonzero deflections.

Results are obtained for isotropic and ±45 deg laminated composite plates with a balanced and symmetric layup. The isotropic results apply to isotropic metal or composites with quasi-isotropic layup. The ±45 deg laminate results apply to graphite-epoxy filamentary material with properties given by the dimensionless quantities

$$\frac{D_{12}+2D_{66}}{\sqrt{D_{11}D_{22}}} = 2.28$$

$$\frac{A_{11}A_{22}-A_{12}^2-2A_{12}A_{66}}{2A_{66}\sqrt{A_{11}A_{22}}} = -0.431$$

For the isotropic plate, both of these quantities are unity and for both the isotropic and ±45 deg laminate plates,

$$A_{22}D_{11}/A_{11}D_{22} = 1$$

These parameters are discussed in Ref. 3.

Results and Discussion

Characteristic load displacement curves for the postbuckling behavior of long isotropic and ±4 deg laminated composite plates with long edges simply supported and held straight are plotted in Figs. 2 and 3. The average compressive stress intensity coefficient is plotted as a function of the applied compressive displacement coefficient in Fig. 2. The average shear stress intensity coefficient is plotted as a function of the applied shear displacement coefficient in Fig. 3. The slope of these curves indicates that the isotropic plate is stiffer than the ±45 deg laminate in the postbuckling range for shear, but that the ±45 deg laminate is slightly stiffer than the isotropic plate for compression. The compression results of Fig. 2 differ from those reported in Ref. 3, since the in-plane boundary conditions are not the same. No shear results for a long plate are available elsewhere.

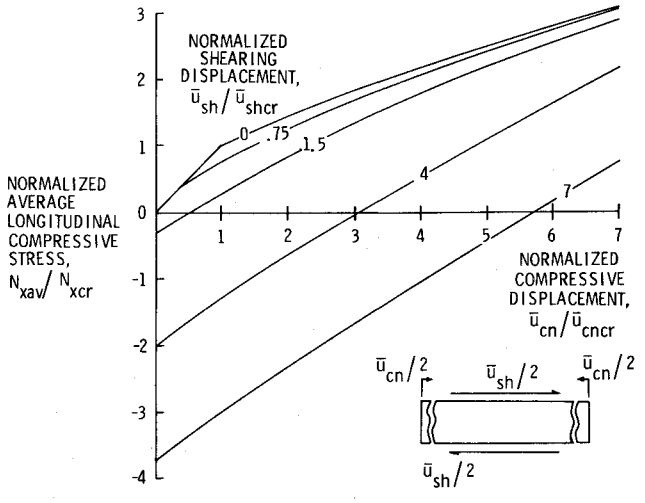

Fig. 6 Average longitudinal compressive stress for an isotropic simply supported plate with edges straight subject to compressive and shearing displacements.

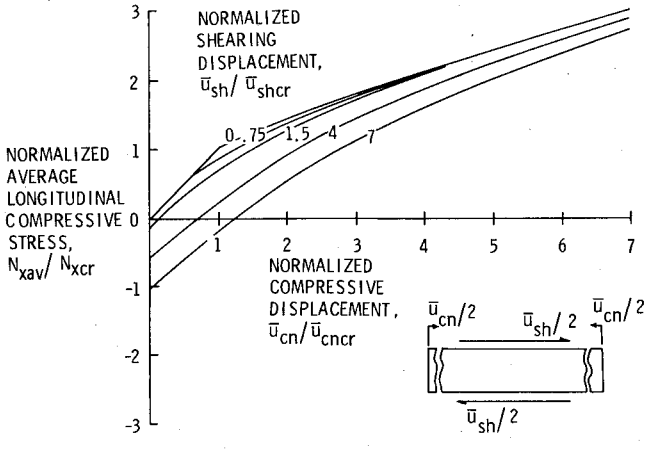

Fig. 7 Average longitudinal compressive stress for a ±45 deg laminated composite simply supported plate with edges straight subject to compressive and shearing displacements.

In-plane boundary conditions are very important for the shear loading case beyond initial buckling. In the present case, with N_y zero on the average (but no applied compressive displacement in the x direction), tensile stresses of the same magnitude as the shear stresses appear in the x direction in the postbuckling range. If a plate in shear is, instead, enclosed in a frame for testing purposes, N_y as well as N_x stresses would appear and the characteristic curve would change; the slope of the characteristic curve would be expected to increase considerably. Such considerations require a careful choice of the in-plane conditions when using the theory.

The magnitude of the average shear stress developed with combinations of applied shearing and compressive displacements is shown in Fig. 4 for the isotropic plate and in Fig. 5 for the ±45 deg laminate. The curve for zero compressive displacement is the same as the corresponding curve of Fig. 3, except that the values of the average shear stress and the shearing displacement are normalized by their critical values for shearing alone. The values of the compressive displacement are similarly normalized by their critical values for compression alone.

As shown in Figs. 4 and 5, shear stresses develop from near zero with or without applied compressive displacements. No bifurcation point exists in the characteristic shear curves for applied compressive displacement greater than its critical value for compression alone. The curves show that the

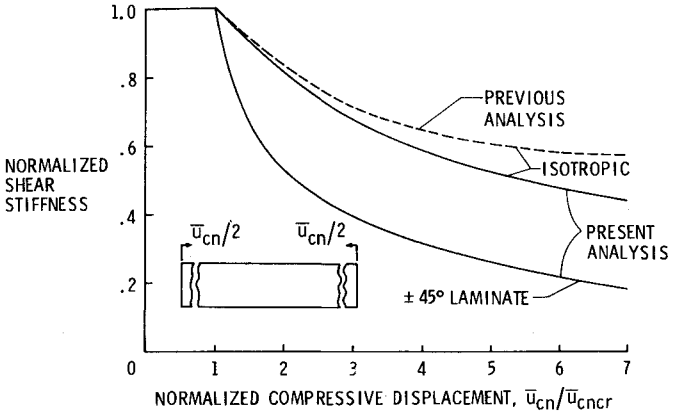

Fig. 8 Stiffness in shear of a plate buckled in longitudinal compression.

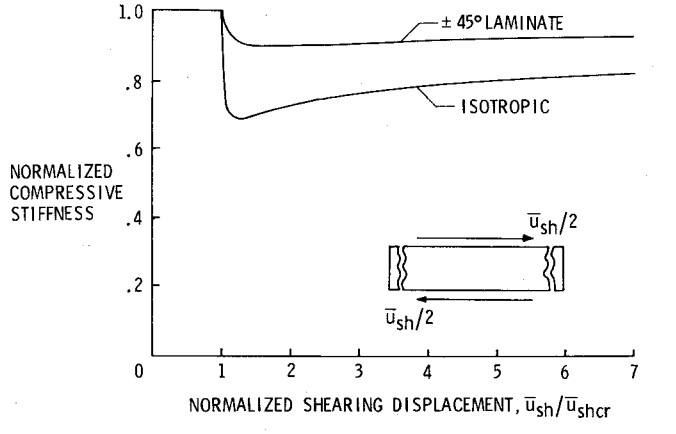

Fig. 9 Stiffness in longitudinal compression of a plate buckled in shear.

decrease in shear stress with the increase in applied compressive displacement is greater for the ±45 deg laminate than for the isotropic plate. As mentioned previously, tensile stresses develop in the longitudinal direction due to shear. With the increase in compressive displacements, these stresses will become smaller and, for large enough compressive displacements, these longitudinal stresses will become compressive as shown in Figs. 6 and 7.

The magnitude of the average longitudinal compressive stress developed with combinations of applied longitudinal compressive and shearing displacements is shown in Fig. 6 for the isotropic plate and in Fig. 7 for the ±45 deg laminate. The curve for zero shear displacement is the same as the corresponding curve of Fig. 2, except that the values are again normalized by their critical values. As discussed in the previous paragraph and shown in Fig. 6, tensile stresses much larger than the critical compressive stress are developed as the shear displacement increases for the isotropic plate. The curves of Fig. 7 show that the tensile stresses which develop for the ±45 deg laminate are not as large as those shown in Fig. 6 for the isotropic plate and that the curves for the compressive stress are much closer together. As shown in Figs. 6 and 7, no bifurcation points appear in these characteristic curves for applied shear displacement greater than the critical value of the shear displacement for shear alone. However, if tensile displacements are applied, bifurcation points in this range will appear.

The shear stiffness of a plate already buckled in compression is important to designers. Shear stiffness calculations have been made at various postbuckling values of the applied compressive displacement. For a given compressive displacement, a small shearing displacement (2% of the value of the critical shearing displacement for shear alone) is applied and

the resulting average shearing stress is calculated. Using this average shearing stress and the applied shearing displacement, an average shear stiffness is determined and this stiffness is normalized using the stiffness prior to buckling. The normalized shear stiffness as a function of normalized compressive displacements is presented in Fig. 8 for isotropic and ±45 deg laminated plates. Also shown is the curve for the stiffness of an isotropic plate from Ref. 15. The trends appear to be the same in the previous results as for the present results; however, for larger compressive displacement, the curve of Ref. 15 reaches a minimum, while the present results continue to decrease. The differences are due to the approximations made in the previous analysis. The stiffness for the ±45 deg laminate is much lower than for the isotropic plate.

The calculated normalized stiffness in compression of a plate already buckled in shear is presented in Fig. 9 as a function of normalized shear displacement. This stiffness is also important in design since it identifies the sensitivity of the buckled plate to a different kind of load. For a given applied shearing displacement, a small compressive displacement (2% of the value of the critical compressive displacement for compression alone) is applied and the resulting average compressive stress is calculated. Using the average compressive stress and the applied compressive displacement, an average compressive stiffness is determined and this stiffness is normalized using the plate compressive stiffness prior to buckling. Results are presented in Fig. 9 for isotropic and ±45 deg laminated plates. The compressive stiffness for the ±45 deg laminate is higher than that for isotropic plates; but, for the shear stiffness of a plate buckled in compression (Fig. 8), the ±45 deg laminate stiffness was lower than the isotropic results. The increase is compressive stiffness with the increase in applied shear displacement is probably due to the large tensile stresses developed in shear.

Conclusions

This paper presents a method of analysis and postbuckling results for a long orthotropic plate loaded in combined compression and shear. Results are also presented for long orthotropic plates in shear alone and in longitudinal compression alone. Characteristic load displacement curves are presented for isotropic and ±45 deg laminated composite plates where the average stress is plotted as a function of the corresponding applied displacement. These curves indicate that, as the displacement increases, the stiffness of the isotropic plate is larger than that for the ±45 deg laminate for shear, but the stiffness of the ±45 deg laminate is slightly larger than that of the isotropic plates for compression. Under shear loading, the plate tends to shorten longitudinally and in-plane restrictions on the plate cause large longitudinal tensile stresses to occur, indicating that the results in shear are dependent to a great extent on the in-plane boundary conditions. Results for shear alone and for combined loading indicate that the longitudinal tensile stresses which develop in the postbuckling range are larger for the isotropic plate than for the ±45 deg laminated plate.

Results are also presented for the shear stiffness of plates buckled in compression and for the compressive stiffness of plates buckled in shear. The ±45 deg laminated plate has a lower stiffness in shear than the isotropic plate for plates already buckled in compression at a given level compared to the critical value. For plates buckled in shear at a given level compared to the critical value, the ±45 deg laminated plate is stiffer in compression than the isotropic plate.

The method of analysis presented in this paper is based on choosing the important terms in a trigonometric series for the deformations in the long direction and then deriving ordinary nonlinear differential equations. Solution of the ordinary differential equation determines the coefficients of the series delineating the behavior in the short direction. Thus, a Levy-type solution is developed for the postbuckling analysis of long plates.

References

[1]Johns, D. J., "Shear Buckling of Isotropic and Orthotropic Plates—A Review," British Aeronautical Research Council, R&M 3677, 1970.

[2]Almroth, B. O. and Brogan, F. A., "The STAGS Computer Code," NASA CR 2950, 1978.

[3]Stein, M., "Postbuckling of Orthotropic Composite Plates Loaded in Compression," AIAA Paper 82-0778, 1982.

[4]Lentini, M. and Pereyra, V., "An Adaptive Finite Difference Solver for Nonlinear Two-Point Boundary Problems with Mild Boundary Layers," *SIAM Journal of Numerical Analysis*, Vol. 14, March 1977.

[5]Ashton, J. E. and Love, T. S., "Shear Stability of Laminated Anisotropic Plates. Composite Materials: Testing and Design," ASTM STP 460, 1969, pp. 352-361.

[6]Housner, J. M. and Stein, M., "Numerical Analysis and Parameter Studies of the Buckling of Composite Orthotropic Compression and Shear Panels," NASA TN D-7996, 1975.

[7]Levy, S., Fienup, K. L., and Wolley, R. M., "Analysis of Square Shear Web Above Buckling Load," NACA TN 962, 1945.

[8]Levy, S., Wolley, R. M., and Corrick, J. N., "Analysis of Deep Rectangular Shear Web Above Buckling Load," NACA TN 1009, 1946.

[9]Stein, M., "The Phenomenon of Change in Buckle Pattern in Elastic Structures," NASA TR R-39, 1959.

[10]Stein, M., "Loads and Deformations of Buckled Rectangular Plates," NASA TR R-40, 1959,

[11]Kaminski, B. E. and Ashton, J. E., "Diagonal Tension Behavior of Boron-Epoxy Shear Panels," *Journal of Composite Materials*, Vol. 5, 1971, p. 553.

[12]Stein, M. and Starnes, J. H. Jr., "Numerical Analysis of Stiffened Shear Webs in the Postbuckling Range," ASME AMD, Vol. 6, 1973, p. 211.

[13]Agarwal, B. L., "Postbuckling Behavior of Composite Shear Webs," *AIAA Journal*, Vol. 19,, July 1981, pp. 933-939.

[14]Southwell, R. V. and Skan, S. W., "On the Stability Under Shearing Forces of a Flat Elastic Strip," *Proceedings of the Royal Society of London*, Ser. A, Vol. 105, No. 733, May 1, 1924, pp. 582-587.

[15]Stein, M., "Behavior of Buckled Rectangular Plates," *Journal of Engineering Mechanics Division*, ASCE, April 1960.